



Synthesis, Optical Characterization And Electrochemical Properties Of Cd_(1-x)Ni_(x)S/ Reduced Graphene Oxide Nanocomposites

Mani Jayanthi^{1,2}, Thirugnanam Lavanya³, SriRangarajan Chenthamarai⁴, Kaveri Satheesh^{5*}

¹Department of Physics, Anna Adarsh College for Women, Chennai, India - 600 040

²Periyar University, Salem, India – 636 011

³Department of Physics, IIT Madras, Chennai, India– 600 036

⁴Department of physics, S.D.N.B Vaishnav College for Women, Chennai, India – 600 044

⁵Research and Development, Department of Physics, Dhanalakshmi College of Engineering, Tambaram, Chennai, India – 601 301

Abstract: Cd_(1-x)Ni_(x)S/rGO Composites were synthesized through reflux method. The prepared composite materials were subjected to study the structural, functional groups and transformation of GO to rGO by X- ray diffractometer (XRD), Fourier transform infrared (FTIR) and Raman spectrometer. The presence of elements, binding energies and the transformation were studied by X- ray photoelectron spectroscopy. Thermal properties of as synthesized materials were analyzed by thermogravimetric analysis. An introduction of Ni ions into CdS/rGO composites results increase in integral area and current, which is analyzed by cyclic voltammetry. This composite will be useful in future optoelectronics and energy storage applications.

Keywords: Cd_(1-x)Ni_(x)S/rGO, composites, Reflux method, Optical properties, Electrochemical property.

Introduction

Graphene, a one-atom thick sheet of sp²-bonded carbon atoms tightly packed into a two-dimensional honeycomb hexagonal benzene ring-like structure has attracted tremendous attention in both the experimental and theoretical scientific interest recently because of its outstanding mechanical property, superior electrical conductivity and mobility, theoretically high specific surface area, excellent optical transmittance, and high chemical stability^{1,2}. Considering the integrative unique nanostructure and extraordinary properties of graphene has aroused tremendous attention for, the entry of graphene into the field of electrochemistry. These unique and intriguing features make this highly versatile graphene possess great potentials in electronics, optoelectronics, chemical sensors, electrochemical capacitors, and catalysis^{3,4}. To harness the potential application of graphene-based materials such as polymer, metal nanoparticles, and semiconductor nanocrystals (NCs)⁵, has great interest in nowadays devoted to graphene-based nanocomposites for developing high performance of electrochemical devices due to the electronic transport property of graphene. Particularly, binary semiconductor nano Crystals, such as CdS, ZnS, CdSe, and CdTe

have been successfully incorporated with graphene or reduced graphene oxide (rGO) by various methods to enhance the electrochemical performance. When graphene is hybridized with cds, graphene can boost the separation and transfer of charge carriers and extremely efficient to promoted the charge transfer within the composite.

Semiconducting nanoparticles have revealed appreciable structural, optical, electrical, luminescence and photocatalytic properties than the bulk structures. II – VI semiconductor materials are important for the fabrication of optoelectronic devices like light emitting diodes (LED), solar cells, laser diodes, photocatalytic and photoconductive cells, etc. Ni doped CdS have been successfully synthesized and their structural, optical and magnetic properties were reported^{6,7}. The defect structure of Ni doped CdS were reported⁸. Herein, we reported a novel Ni doped CdS embedded on reduced graphene oxide sheets. nanocomposite which was in a chemical synthesis and showed their interactive effect markedly enhanced electrochemical performance composites in comparison with CdS/rGO alone.

Experimental Procedure

Synthesis of Graphite Oxide and Cd_(1-x)Ni_(x)S/rGO Composites

Graphite oxide is synthesized by modified Hummers Method⁹. Cadmium acetate, Nickel nitrate hexa hydrate and thiourea were used to synthesize the composite. All the chemicals were used as received. 100 mg of graphite powder was added to the dehydrated ethanol followed by ultrasonication for one hour to obtain the homogeneous dispersion of graphene oxide. Then the graphene oxide dispersion is used for further reaction. 0.5 mol.% of Cadmium acetate, 0.5 mol.% of thiourea and (5 to 20 wt%) Nickel nitrate hexahydrate were added to the graphene oxide solution under stirring. The reaction was performed at 60°C for 24 hours. The precipitate was washed and filtered by ethanol and water three times, dried in a vacuum oven at 60°C for 12 hours. Finally, the powders were calcined at 250°C for 5 hours.

Characterization Studies

The structure of the synthesized materials were recorded by powder X-ray diffraction (XRD) using Rigaku Rintz Ultima+ with CuK α radiation ($\lambda=1.54056\text{nm}$) at the scanning rate of 1°min^{-1} . The voltage and electric current were chosen as 40kV and 40 mA respectively. Raman Spectra were carried out using Horiba-Jobin Yuon instrument with a 514 nm (Green laser) in the range 100 cm^{-1} to 2000 cm^{-1} . The morphology and structure of the composites were examined through Transmission electron microscopy (TEM-JEOL JEM 2100). Fourier transform infrared (FT-IR) study was performed by Perkin Elmer (spectrum 100 FTIR spectrometer) using a KBr pellets in the frequency range 4000 cm^{-1} to 400 cm^{-1} . Thermal properties of samples were analyzed by Thermogravimetry (TG) analysis using SII EXSTAR 6000 with TG/DTA6200 thermogravimetric analyzer from 40 to 1000°C at the heating rate of $5^\circ \text{C}/\text{min}$ using sealed platinum pans under N_2 flow. The presence of the element in the composite material was analyzed by X-ray photoelectron spectroscopy, recorded on Theta Probe- Thermo Fisher scientific Inc X-ray photoelectron spectrometer. Electrochemical experiments were carried out by using BIO LOGIC instrument with a three electrode system with glassy carbon electrode as the working electrode, platinum wire as the counter electrode and Ag/AgCl as the reference electrode.

Results and Discussion

Powder XRD Analysis

XRD patterns of the composites were recorded to confirm the phase and structure of the material. Fig 1 Shows the XRD pattern of the graphite oxide, a peak at 11.7° corresponding to the (002) plane and well agree with the earlier report. All diffraction peaks appeared at $2\theta = 26.5^\circ$, 43.9° and 52.0° could be indexed to the planes (111), (220) and (311) cubic phase of the CdS (JCPDS 80-0019), respectively (Fig.1b). When the Ni ions concentration increases in composite materials, the peaks gets broadening and shift towards to the lower angle side (Figures 1c-1f). Because, the ionic radii of Ni ions (0.069 nm) is less than Cd ions (0.097 nm). Increase of Ni ions does not affect the cubic phase of CdS nanoparticles. The disappearance of the GO peak in the low angle region could not be found in the composite materials, indicating the CdS/rGO exhibit a peak at $2\theta = 26.5^\circ$ which result the overlap of diffraction peaks from the (002) plane of rGO and the (111) plane of cubic

CdS. The other two diffraction planes of CdS, (220) and (311) were too weak to be identified due to the very small quantity of CdS nanoparticles adsorbed on rGO sheets.

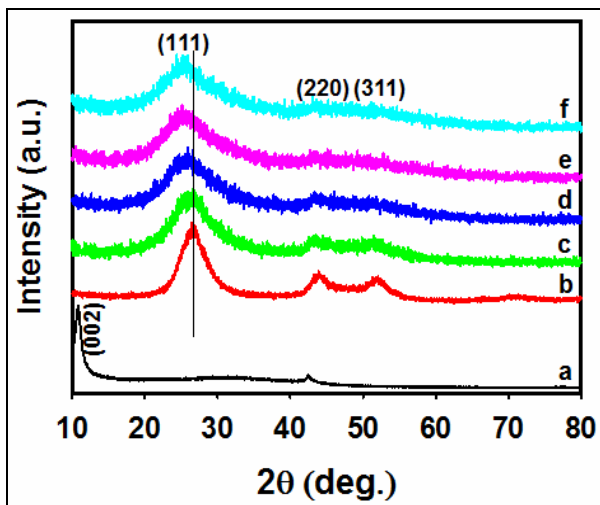


Fig. 1 XRD patterns of (a) GO, (b) CdS/rGO, (c) Cd_{0.95}Ni_{0.05}S/rGO, (d) Cd_{0.90}Ni_{0.10}S/rGO, (e) Cd_{0.85}Ni_{0.15}S/rGO and (f) Cd_{0.80}Ni_{0.20}S/rGO composites

FT-IR Spectroscopy Analysis

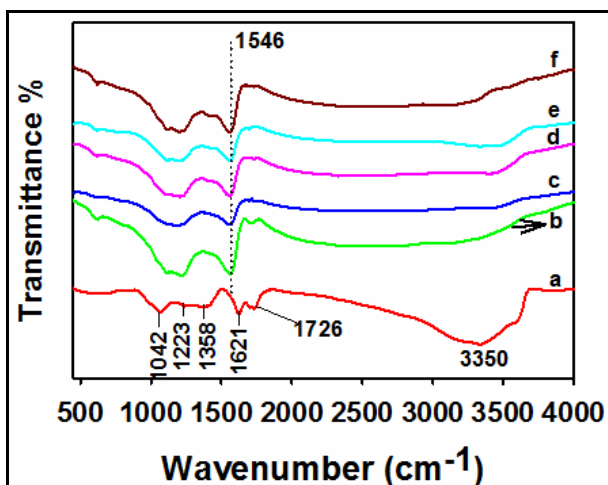


Fig. 2 FT-IR spectra of (a) GO, (b) CdS/rGO, (c) Cd_{0.95}Ni_{0.05}S/rGO, (d) Cd_{0.90}Ni_{0.10}S/rGO, (e) Cd_{0.85}Ni_{0.15}S/rGO and (f) Cd_{0.80}Ni_{0.20}S/rGO composites

The FT-IR spectrum of GO and the composite material is shown in Fig. 2. The GO (Fig. 2a) spectrum, broad absorption peak at 3350 cm⁻¹ is due to stretching vibrations of hydroxyl groups. The oxygen containing functional groups were observed in the GO spectra at 1042 cm⁻¹, 1223 cm⁻¹, 1358 cm⁻¹, 1621 cm⁻¹ and 1726 cm⁻¹ corresponds to the C-O stretching vibrations, stretching vibration peak of C-OH, deformation peak of C-O-H, skeletal ring vibrations of unoxidized graphitic domains and C=O stretching of COOH groups are situated at graphite oxide sheet edges, respectively. Compared to GO spectrum, the spectra of composite material (Fig. 2b – 2f) show the absence of carboxyl group at 1726 cm⁻¹ and hydroxide group 1358 cm⁻¹, other functional groups remained unvaried, indicates that the GO is converted to rGO. The peak appears at 1546 cm⁻¹ attributed to the skeletal vibrations of graphene sheets¹⁰. The peak at 614 cm⁻¹ is due to the C-S vibrations of CdS nanoparticles¹¹. This result provides an evidence for the presence of both CdS and rGO sheets in the composites.

Raman Spectroscopy Analysis

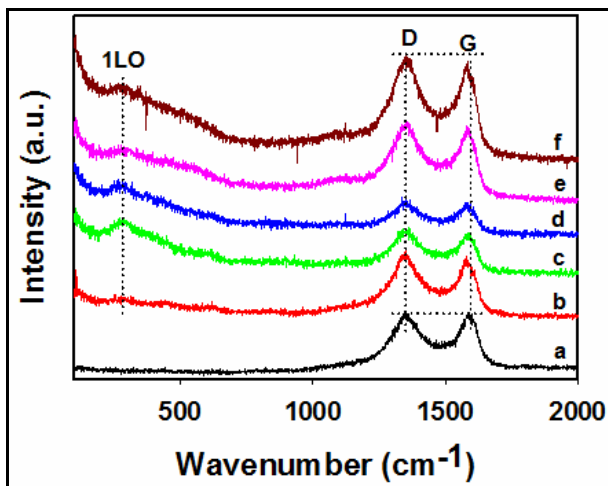


Fig. 3 Raman spectra of (a) GO, (b) CdS/rGO, (c) Cd_{0.95}Ni_{0.05}S/rGO, (d) Cd_{0.90}Ni_{0.10}S/rGO, (e) Cd_{0.85}Ni_{0.15}S/rGO and (f) Cd_{0.80}Ni_{0.20}S/rGO composites

Raman spectroscopy was employed to probe functionalized carbon materials directly for strong sensitivity to the electronic structure of the samples. Fig. 3 shows the Raman spectra for GO, CdS/rGO and Cd_(1-x)Ni_(x)S/rGO composites. The Raman spectrum of GO (Fig. 3a) shows the G band at 1591 cm⁻¹ and D band at 1350 cm⁻¹. For the composite materials (Fig. 3b – 3f) of Raman spectrum shows the shift in G band downwards in the wavenumber from 1591 cm⁻¹ to 1584 cm⁻¹, which might be caused by the increasing number of layers in their solid states and slight increase in an intensity D/G ratio was higher than that for GO was also observed, indicating that the reduction process introduced a considerable amount of structural defect in the graphene lattice. This is a common phenomenon in the Raman spectra of reduced GO¹². This result provides an evidence for the formation of both CdS and rGO in the composites and the successful transformation from GO to rGO reduced by thiourea.

Thermogravimetric Studies

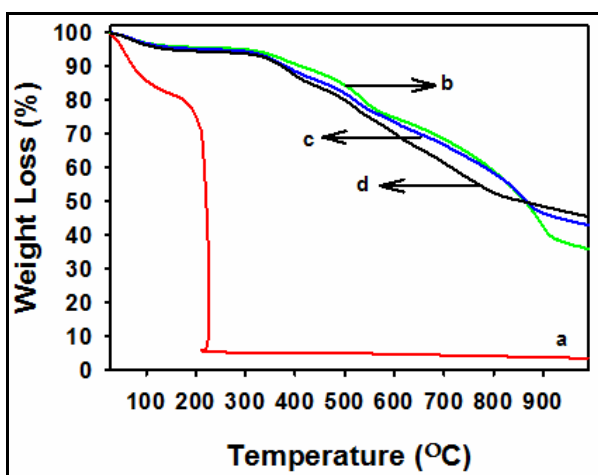


Fig. 4 TGA curves of (a) GO, (b) CdS/rGO, (c) Cd_{0.90}Ni_{0.10}S/rGO and (d) Cd_{0.80}Ni_{0.20}S/rGO composites

The thermal property of GO, CdS/rGO, Cd_{0.90}Ni_{0.10}S/rGO and Cd_{0.80}Ni_{0.20}S/rGO composites were characterized by thermogravimetric analysis, which was performed in nitrogen atmosphere with a heating rate of 5°C min⁻¹. Fig. 4 show the TGA curve of GO, which shows the weight loss below 100°C, which is due to the removal of absorbed water molecules and the major weight loss is around at 200°C may be attributed to the removal of oxygen containing functional groups. Fig. 4b show the TGA curve of CdS/rGO, with increasing the

temperature of the composites show a gradual weight loss upto 800°C, which is well agree with earlier report ⁶. After 800°C, an abrupt weight loss occurs at around 910°C, which results from the decomposition of CdS. Fig. 4c and 4d shows the TGA curves of Cd_{0.90}Ni_{0.10}S/rGO and Cd_{0.80}Ni_{0.20}S/rGO composites, respectively. These materials also show the gradual weight loss upto 800°C. After 800°C, confirming the good thermal stability than CdS/rGO composites. From these observations, when the Ni ions concentration increased, the composite materials show the good thermal stability up to 1000°C.

X-ray Photoelectron Spectroscopy Analysis

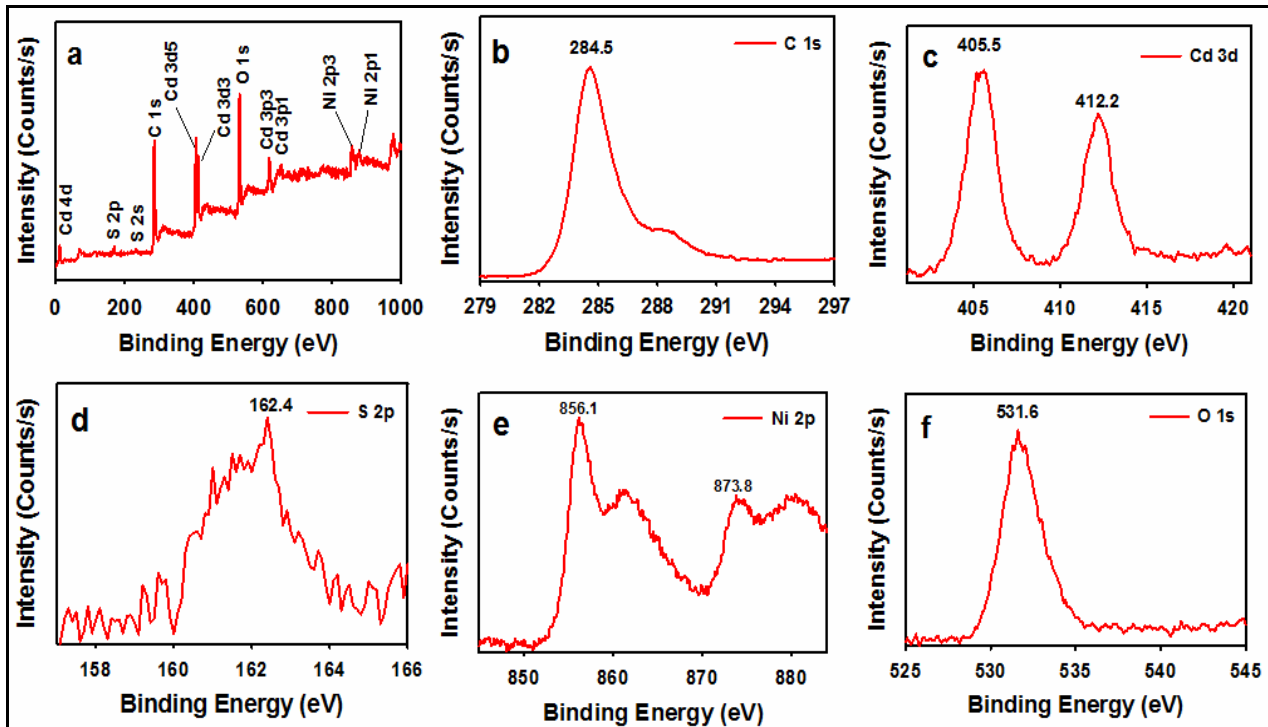


Fig. 5 X-ray photoelectron spectra of Cd_(0.80)Ni_(0.20)S/rGO composite (a) survey, (b) C 1s, (c) Cd 3d, (d) S 2p, (e) Ni 2p and (f) O 1s

X-ray photoelectron spectroscopy (XPS) were used to confirm the formation of rGO from GO during the thiourea assisted reflux method treatment (Fig. 5). The identified peaks were labeled to various corresponding elements. Fig. 5 shows the full XPS spectra taken from the surface of the Cd_(1-x)Ni_(x)S/rGO composite. The peaks in the XPS data for all composites could be identified to originate from Cd, S, Ni, C, and O elements. The C1s peak of Cd_(1-x)Ni_(x)S/rGO nanocomposite was obviously decreased as compared to that of GO in the wide region, suggesting that most of the oxygen-contained functional groups were successfully reduced.

TEM Analysis

The morphology of the Cd_(1-x)Ni_(x)S/rGO composites were characterized by TEM. Fig. 6 and 7 show the TEM and HRTEM images Cd_(1-x)Ni_(x)S/rGO composite material. Inset in the HRTEM images shows the corresponding SAED patterns with three fold rings, which confirms the cubic CdS nanoparticles. The images shows the multilayer rGO sheets decorated by the Cd_(1-x)Ni_(x)S nanoparticles. The Cd_(1-x)Ni_(x)S particles were well aggregated were observed in TEM images.

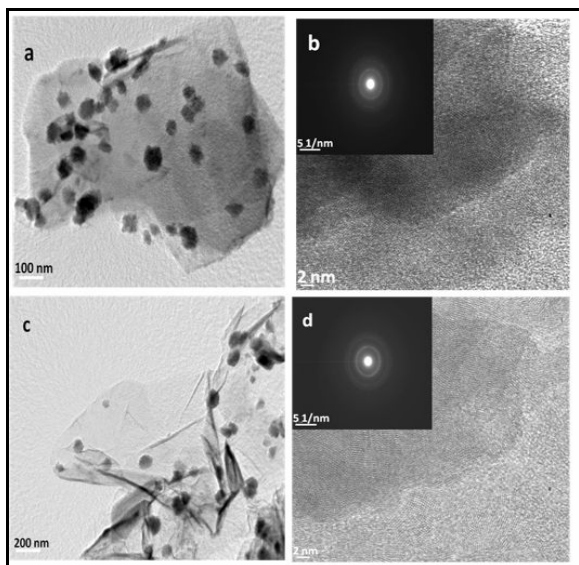


Fig. 6 TEM and HRTEM images of (a & b) $\text{Cd}_{(0.95)}\text{Ni}_{(0.05)}\text{S/rGO}$ and (c & d) $\text{Cd}_{(0.90)}\text{Ni}_{(0.10)}\text{S/rGO}$ composites. Inset in the HRTEM images show the corresponding SAED patterns

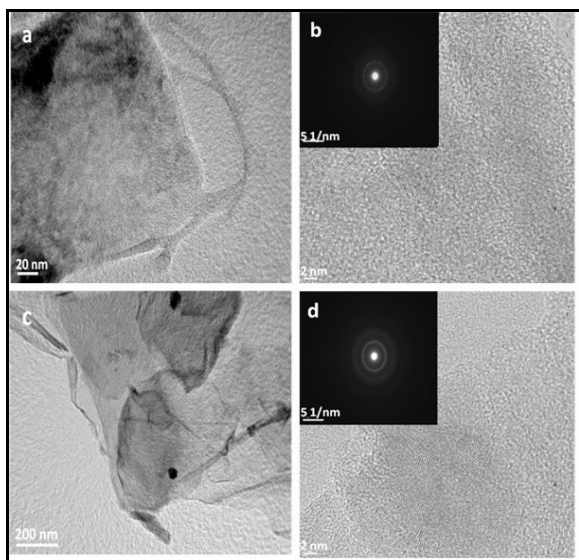


Fig. 7 TEM and HRTEM images of (a & b) $\text{Cd}_{(0.85)}\text{Ni}_{(0.15)}\text{S/rGO}$ and (c & d) $\text{Cd}_{(0.80)}\text{Ni}_{(0.20)}\text{S/rGO}$ composites. Inset in the HRTEM images show the corresponding SAED patterns

Electrochemical Studies

Potassium ferrocyanide solution was used to evaluate the electrochemical behavior of $\text{Cd}_{(0.90)}\text{Ni}_{(0.10)}\text{S/rGO}$ and $\text{Cd}_{(0.80)}\text{Ni}_{(0.20)}\text{S/rGO}$ modified electrodes. Fig. 8C compares the Cyclic Voltammetry (CV) curves of $\text{Cd}_{(0.90)}\text{Ni}_{(0.10)}\text{S/rGO}$ and $\text{Cd}_{(0.80)}\text{Ni}_{(0.20)}\text{S/rGO}$ modified electrode in the aqueous solution of 5mM ferricyanide, 5 mM ferrocyanide and 0.1 M KNO_3 . The weights of the electrocatalysts were controlled to be the same on each electrode. Every CV cycle does not show a couple of oxidation and reduction peaks due to the redox reaction of $\text{Fe}^{3+}/\text{Fe}^{2+}$. It is very clear from the CV curves and TEM images, in the composites rGO sheets composition is high when compared to the CdS/rGO composites. The Cv peak currents of two modified electrodes are higher than the CdS/rGO composites. The influence of the scan rates on the CV performance of the $\text{Cd}_{(0.90)}\text{Ni}_{(0.10)}\text{S/rGO}$ and $\text{Cd}_{(0.80)}\text{Ni}_{(0.20)}\text{S/rGO}$ composite is shown in Fig 8a and 8b.

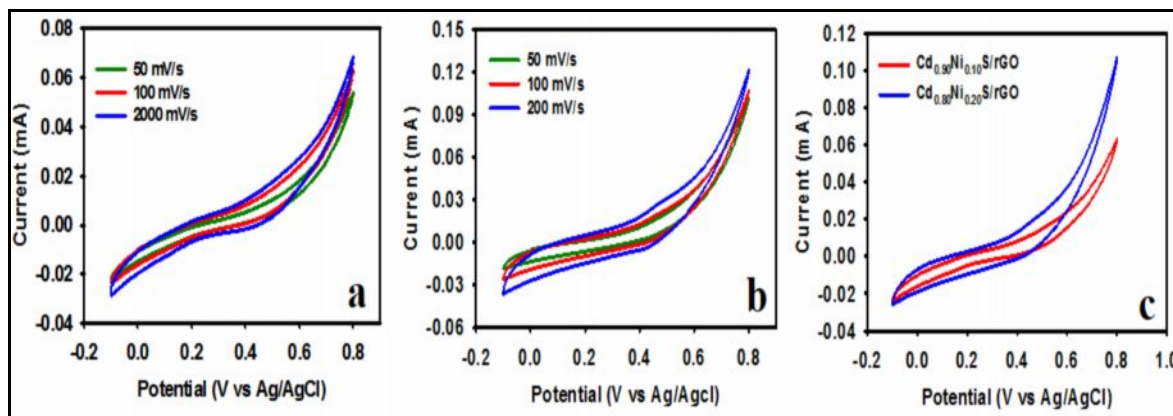


Fig. 8 CV curves of $\text{Cd}_{(0.90)}\text{Ni}_{(0.10)}\text{S/rGO}$ modified electrode at different scan rates: 50 mV/s, 100 mV/s and 200 mV/s (b) $\text{Cd}_{(0.80)}\text{Ni}_{(0.20)}\text{S/rGO}$ modified electrode at different scan rates: 50 mV/s, 100 mV/s and 200 mV/s (c) Comparative CV curves of $\text{Cd}_{(0.90)}\text{Ni}_{(0.10)}\text{S/rGO}$ and $\text{Cd}_{(0.80)}\text{Ni}_{(0.20)}\text{S/rGO}$ modified electrode at a scan rate of 100 mV/s

Conclusion

$\text{Cd}_{(1-x)}\text{Ni}_{(x)}\text{S/rGO}$ composites have been synthesized by a reflux method. Thiourea acts as an efficient reduction as well as sulfide source. XRD, FTIR, Raman, XPS and CV techniques were used to characterize the structure, surface morphology, elements presence and electrochemical behavior of the materials. The integration of the transition metal (Ni) doped inorganic semiconducting nanoparticle with the conductive reduced GO sheets opens a new route for the development of novel materials including, fuel cell electrode materials and applications such as solar energy conversion, photovoltaic devices and electrochemical catalysts.

References

1. Lu T, Zhang R, Hu C, Chen F, Duo S and Hu Q., TiO_2 -graphene composites with exposed {001} facets produced by a one-pot solvothermal approach for high performance photocatalyst, *Phys. Chem. Chem. Phys.*, 2013,15, 12963-12970.
2. Mo Z, Liu P, Guo R, Deng Z, Zhao Y, and Sun Y., Graphene sheets/ Ag_2S nanocomposites: Synthesis and their application in supercapacitor materials, *Mat. Lett.*, 2012, 68, 416-418.
3. Cao M, Wang P, Ao Y, Wang C, Hou J, and Qian J., Photocatalytic degradation of tetrabromo bis phenol A by a magnetically separable graphene- TiO_2 composite photocatalyst: Mechanism and intermediates analysis, *Chem. Eng. Jour.*, 2015, 264, 113-124.
4. Satheesh. K. and Jayavel. R., Synthesis and electrochemical properties of reduced graphene oxide via chemical reduction using thiourea as a reducing agent, *Mat. Lett.*, 2013, 113, 5-8.
5. Lavanya. T, Satheesh. K, Dutta. M, Jaya. N.V, and Fukata. N., Superior photocatalytic performance of reduced graphene oxide wrapped electrospun anatase mesoporous TiO_2 nanofibers, *J. Alloys and Comp.*, 2014, 615, 643-650.
6. Rmili A, Ouachtari F, Bouaoud A, Louardi A, Chtouki T, Elidrissi B, and Erguig H., Structural, optical and electrical properties of Ni-doped CdS thin films prepared by spray pyrolysis, *J. Alloy. and Comp.*, 2013, 557, 53-59.
7. Chandramohan S, Strache T, Sarangi S.N, Sathyamoorthy R, and Som, T., Influence of implantation induced Ni-doping on structural, optical, and morphological properties of nanocrystalline CdS thin films, *Mater. Sci. and Eng. B.*, 2010, 171, 16-19.
8. Zheng W.C, He L, Li W, and Liu H.G, Research on the spin- Hamiltonian parameters and defect structure for Ni^{2+} ion in CdS, *Physica B.*, 2013, 412, 1-3.
9. Satheesh K, Lavanya T, Mrinal D, Jayavel R. and Naoki F., Thiourea assisted one-pot easy synthesis of CdS/rGO composite by the wet chemical method: Structural, optical, and photocatalytic properties, *Ceramics Int.*, 2013, 39, 9207 – 9214.
10. Xu Y.X, Bai H, Lu G.W, Li C, and Shi G.Q., Flexible graphene films via the filtration of water-soluble non covalent functionalized graphene sheets, *J. of Amer. Chem. Soc.*, 2008, 130, 5856–5857.

11. Stankovich. S, Dikin D.A, and Piner R.D., Synthesis of graphene - based nanosheets via chemical reduction of exfoliated graphite oxide, *Carbon* , 2007, 45, 1558–1565.
12. Wang H.L, Robinson J.T, Li X.L, and Dai H.J., Solvothermal reduction of chemically exfoliated graphene sheets, *J. Am. Chem. Soc.*, 2009, 131, 9910-9916.
